Robust Metal−Organic Framework with An Octatopic Ligand for Gas Adsorption and Separation: Combined Characterization by Experiments and Molecular Simulation

Wenjuan Zhuang,[†] Daqiang Yuan,[†] Dahuan Liu,[‡] Chongli Zhong,[‡] Jian-Rong Li,[†] and Hong-Cai Zhou*,[†]

[†]Department of Chemistry, Texas A&M University, College Station, Texas 77843, United States

[‡]Lab of Computational Chemistry, Department of Chemical Engineering, Beijing University of Chemical Technology, Beijing, 100029, China

S *Supporting Information*

ABSTRACT: A newly designed octatopic carboxylate ligand, tetrakis[(3,5-dicarboxyphenyl)oxamethyl]methane (TDM^{8-}) has been used to connect a dicopper paddlewheel building unit affording a metal−organic framework (MOF), $Cu_4(H_2O)_4(TDM)·xS$ (PCN-26·xS, S represents noncoordinated solvent molecules, PCN = porous coordination network) with novel structure, high gas uptake, and interesting gas adsorption selectivity. PCN-26 contains two different types of cages, octahedral and cuboctahedral, to form a polyhedron-stacked three-dimensional framework with open channels in three orthogonal directions. Gas adsorption studies of N_2, Ar, and H_2 on an activated PCN-26 at 77 K, 1 bar, reveals a Langmuir surface area of 2545 m^2/g, a Brunauer−Emmett−Teller (BET) surface area of 1854 m^2/g, a total pore volume of 0.84 cm^3/g, and a H_2 uptake capacity of 2.57 wt %. Additionally, PCN-26 exhibits a CO_2/N_2 selectivity of 49:1 and CO_2/CH_4 selectivity of 8.4:1 at 273 K. To investigate properties of gas adsorption and the adsorption sites for CO_2 in activated PCN-26, theoretical simulations of the adsorption isotherms of CO_2, CH_4, and N_2 at different temperatures were carried out. Experimental results corroborate very well with those of molecular simulations.
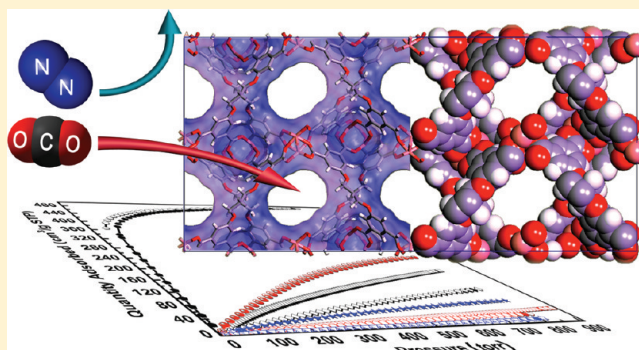
KEYWORDS: metal−organic framework, octatopic carboxylate ligand, gas adsorption and separation, molecular simulation

INTRODUCTION

Metal−organic frameworks (MOFs)[1−5] have become one of the fastest growing research fields in chemistry over the past two decades.[6−9] The motivation comes from not only their tunable pore-size, adjustable surface, and intriguing structural diversity,[10,11] but also their tantalizing potential applications such as gas storage,[12−16] separation,[17−19] shape/size/enantio-selective catalysis,[20−23] and others.[24−26] By judicious selection of the metals (or clusters) and organic linkers with fixed geometry, a vast variety of MOFs have been assembled with predesigned atom-to-atom connectivity, structural topology, and nondispersed pore size distribution.[27−29]

Rigid aromatic polycarboxylate ligands are a widely used family of organic ligands in the preparation of MOFs, and a large number of MOFs have been successfully constructed by using ditopic,[30−32] tritopic,[15,33,34] tetratopic[9,35−37] or hexatopic[38−40] carboxylate ligands. Octatopic[41,42] carboxylate ligands, on the other hand, are very rare. This can be ascribed to the diverse ligand conformation and steric congestion of an octatopic carboxylate ligand as well as the difficulty in synthesis of such a ligand. However, such an octatopic ligand may help to produce new MOFs with improved porosity and stability.

Herein, we report the synthesis of the acid of a flexible octatopic carboxylate ligand, tetrakis[(3,5-dicarboxyphenyl)-oxamethyl]methane (H_8TDM, scheme 1). H_8TDM reacted with Cu(II) under solvothermal reaction conditions to give a new MOF, $Cu_4(H_2O)_4(TDM)·xS$ (PCN-26·xS, S presents noncoordinated solvent molecules, PCN = porous coordination network), in which a Cu(II) paddle-wheel secondary building unit (SBU) acts as an inorganic node. PCN-26 contains two different types of cages, octahedral and cuboctahedral, to form a polyhedron-stacked three-dimensional framework with open channels in three orthogonal directions. Gas adsorption studies of N_2, Ar, and H_2 on an activated PCN-26 at 77 K, 1 bar, reveals a Langmuir surface area of 2545 m^2/g, a Brunauer−Emmett−Teller (BET) surface area of 1854 m^2/g, a total pore volume of 0.84 cm^3/g, and a H_2 uptake capacity of 2.57 wt %. Additionally, PCN-26 exhibits a CO_2/N_2 selectivity of 49:1 and CO_2/CH_4 selectivity of 8.4:1 at 273 K. To investigate properties of gas adsorption and the adsorption sites for CO_2

Scheme 1. Structure of the Acid of Tetrakis[(3,5-dicarboxyphenyl)oxamethyl]methane, H_8TDM
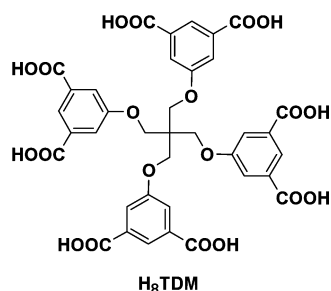
H_8TDM

in activated PCN-26, theoretical simulations of the adsorption isotherms of CO_2, CH_4, and N_2 at different temperatures were carried out. Experimental results corroborate very well with those of molecular simulations.

■ EXPERIMENTAL SECTION

General Information. Commercially available reagents were used as received without further purification. NMR ^{1}H data were collected on a Mercury 300 spectrometer. Thermogravimetry analysis (TGA) was obtained under N_2 atmosphere on a TGA-50 (Shimadzu) thermogravimetric analyzer with a heating rate of 5 °C min^{-1}. The powder X-ray diffraction (PXRD) were recorded on a Bruker D8 Discover diffractometer equipped with a Cu sealed tube (λ = 1.54178 Å) at a scan rate of 0.15 s deg^{-1}, solid-state detector, and a routine power of 1400 W (40 kV, 40 mA). The as synthesized sample was dispersed on low-background quartz discs (G. M. Associates, Inc., Oakland, California) for analysis. The activated sample for powder X-ray diffraction was prepared under nitrogen atmosphere and covered with a Kapton film held with a metric O-ring on a home designed specimen holder (see Figure S1 in the Supporting Information) to avoid contact with air. Simulation of the PXRD spectrum was carried out by the single-crystal data and diffraction-crystal module of the *Mercury* program available free of charge via Internet at http://www.ccdc.cam.ac.uk/products/mercury/.

Synthesis of the Acid of Tetrakis[(3,5-dicarboxyphenyl)-oxamethyl]methane. a. Tetramethyl Tetrakis[(3,5-dimethyl benzoate)oxamethyl]methane. This compound was synthesized following a procedure similar to a literature method.[43] Under a nitrogen atmosphere, a mixture of 1,3-dibromo-2,2-bis(bromomethyl)-propane (3.2 g, 8.25 mmol), dimethyl 5-hydroxyisophthalate (14.0 g, 66.61 mmol), and anhydrous K_2CO_3 (32.0 g, 0.23 mol) in 200 mL of N,N-dimethylformamide (DMF) was heated to 70 °C for 72 h while vigorously stirring. After removal of most of the solvent under reduced pressure, the residue was dissolved in dichloromethane (300 mL) and washed with water. The combined organic phase was dried over $MgSO_4$ and concentrated. The crude product was purified by column chromatography (silica, ethyl acetate/hexanes = 5/5) to afford the white solid of tetramethyl tetrakis[(3,5-dimethyl benzoate)oxamethyl]-methane, 6.1 g (yield, 82%). ^{1}H NMR (300 MHz, DMSO-d^6): δ = 7.94 (s, 4H); 7.67 (s, 8H); 4.46 (s, 8H); 3.85 (s, 24H).

b. Acid of Tetrakis[(3,5-dicarboxyphenyl)oxamethyl]methane, (H_8TDM). Tetramethyl tetrakis[(3,5-dimethyl benzoate)oxamethyl]-methane (6.1 g, 6.7 mmol) and sodium hydroxide (21.6 g, 0.54 mol) were suspended in 300 mL tetrahydrofuran/methanol/water (v/v/v = 1/1/1). The mixture was stirred at room temperature overnight. After removal of the organic solvent under reduced pressure, 20% hydrochloric acid aqueous solution was added to the remaining aqueous solution until the pH value was adjusted to approximately 2. The resulting white precipitate was collected by filtration, washed with water, and dried under vacuum to give white solid of H_8TDM (4.8 g, 90%). ^{1}H NMR (300 MHz, DMSO-d^6): δ = 13.50 (br, 8H); 8.02 (s, 4H); 7.68 (s, 8H); 4.44 (s, 8H).

Synthesis of PCN-26·xS, $Cu_4(H_2O)_4(TDM)$·xS. A mixture of H_8TDM (0.05 g, 6.3 × 10^{-5} mol), $CuBr_2$ (0.15 g, 6.7 × 10^{-4} mol), and 1 mL of tetrafluoroboric acid (HBF$_4$, 48% min w/w aqueous

solution) in 17 mL of dimethylformamide (DMF) was sealed in a 20 mL borosilicate glass scintillation vial and placed in an oven at 60 °C for 72 h. The resulting green crystals of $Cu_4(H_2O)_4(TDM)$·xS (PCN-26·xS, S = noncoordinated solvent molecules) were washed with DMF and collected.

X-ray Crystallography. Single-crystal X-ray data of PCN-26·xS was collected on a Bruker Smart APEX diffractometer equipped with a low temperature device and a fine-focus sealed-tube X-ray source (Mo−Kα radiation, λ = 0.71073 Å, graphite monochromated). The structure was solved by direct methods and refined by full-matrix least-squares on F^2 with anisotropic displacement using the *SHELXTL* software package.[44] Non-hydrogen atoms were refined with anisotropic displacement parameters during the final cycles. Hydrogen atoms on carbon were calculated in ideal positions with isotropic displacement parameters. In PCN-26·xS, free solvent molecules were highly disordered, and attempts to locate and refine the solvent peaks were unsuccessful. The diffused electron densities resulting from these residual solvent molecules were removed from the data set using the *SQUEEZE* routine of *PLATON* and refined further using the data generated.[45] The contents of the solvent region are not represented in the unit cell contents in the crystal data. The details for data collection and refinement are included in the CIF file in the Supporting Information.

Low-Pressure Gas Sorption Measurements. Gas sorption isotherm measurements were performed on an ASAP 2020 Surface Area and Pore Size Analyzer. An as-isolated sample of PCN-26·xS was soaked in methanol for three days to remove the noncoordinated solvent molecules, during the exchange the methanol was refreshed six times. The sample was collected by decanting and treated with dichloromethane similarly to remove methanol solvates. After the removal of dichloromethane by decanting, the wet sample was activated by drying under a dynamic vacuum at room temperature overnight to obtain activated PCN-26 (PCN-26-ac). Before the measurement, the PCN-26-ac sample was dried again by using the "degas" function of the surface area analyzer for 10 h at 80 °C. UHP grade (99.999%) N_2, Ar, H_2, CO_2, and CH_4 were used for all measurements. The temperatures were maintained at 77 K (liquid nitrogen bath), 87 K (liquid argon bath), 195 K (acetone-dry ice bath), 273 K (ice−water bath), or 298 K (room temperature), respectively.

High-Pressure Gas Sorption Measurements. High-pressure H_2 excess adsorption of PCN-26-ac was measured using an automated controlled Sieverts' apparatus (PCT-Pro 2000 from Setaram) at 77 K (liquid nitrogen bath). An activated sample (1.484 g) was loaded into a sample holder under an argon atmosphere. Before the measurements, the sample was degassed at 80 °C overnight. The free volume was determined by the expansion of low-pressure He (<5 bar) at room temperature. The temperature gradient between gas reservoir and sample holder was corrected by applying a correction factor to the raw data, which was obtained by replacing the sample with polished stainless-steel rod and measuring the adsorption isotherm at the same temperature over the requisite pressure regime. The total gas uptake was calculated by: $N_{total} = N_{excess} + \rho_{bulk}V_{pore}$, where ρ_{bulk} equals to the density of compressed gases at the measured temperature and V_{pore} was obtained from the N_2 isotherm at 77 K.[7]

■ COMPUTATIONAL DETAILS

Force Fields. The potential parameters and partial charges for all the adsorbates are shown in Table 1. In this work, H_2 was modeled by a Lennard−Jones (LJ) interaction site located at its center of mass and three partial charges with two located at H atoms and one at the center between two H atoms with bond length of 0.074 nm.[46] CO_2 was modeled as a linear molecule with three charged LJ interaction sites located on each atom with C−O bond length l = 0.116 nm, taken from the TraPPE force field developed by Potoff and Siepmann.[47] CH_4 was modeled as a single LJ interaction site, and the potential parameters were also taken from TraPPE force field, which was able to reproduce the critical parameters and liquid densities of alkanes.[48] A three-site model was used for N_2, with two sites located at two N atoms and the

Table 1. LJ Potential and Coulombic Potential Parameters for the Adsorbates

adsorbate	site	LJ parameters		charge (e)
		σ (nm)	ε/k_B (K)	
H_2	H_2_H	0	0	0.468
	H_2_M	0.296	36.70	−0.936
CO_2	CO_2_O	0.305	79.00	−0.35
	CO_2_C	0.280	27.00	0.70
N_2	N_2_N	0.331	36.00	−0.482
	N_2_M	0	0	0.964
CH_4	CH_4	0.373	148.0	0.0

third one located at its COM site. The bond length between two N atoms is 0.110 nm.[47]

The MOF material studied here was modeled by the atomistic representation. A combination of the site–site LJ and Coulombic potentials was adopted to calculate the interactions between adsorbates and adsorbents. The LJ parameters for the framework atoms in PCN-26-*ac* were taken from Dreiding force field as listed in Table 2.[49] The above set of potential models have been successfully

Table 2. LJ Potential Parameters for the Atoms in the Framework PCN-26-*ac*

LJ parameters	Cu^a	C	O	H
σ (nm)	0.311	0.347	0.303	0.285
ε/k_B (K)	2.517	47.86	48.16	7.65

*a*Taken from the UFF force field[57] (it is missed in the Dreiding force field).

used to describe the adsorption and separation of H_2,[50,51] CO_2,[52,53] CH_4,[54] and N_2[53,55] in PCN-26-*ac*. In this work, atomic partial charges for the frameworks of PCN-26-*ac* (the definition of the types of the atoms in H_8TDM are shown in Scheme S1) were estimated using the CBAC method developed by Zhong's group[53,56] with slight variation to make the total charge to be zero, as shown in Table S1 in the Supporting Information.

$$U_{FH}(r) = U(r) + \frac{\beta\hbar^2}{24\mu}\left[U''(r) + \frac{2U'(r)}{r}\right]$$
$$+ \frac{\beta^2\hbar^4}{1152\mu^2}\left[\frac{15U'(r)}{r^3} + \frac{4U'''(r)}{r} + U''''(r)\right] \quad (1)$$

Considering the adsorption of hydrogen occurred at low temperature, the quartic Feynman-Hibbs (FH) effective potential[58] was used to account for the quantum effects, where U denotes the classical LJ potential, r is the molecule–molecule distance, $\hbar$ is Planck's constant divided by 2π; and the prime, double prime, etc., denote the first-, second-, and higher-order derivatives with respect to r, respectively. The second and third terms in eq 1 are the quantum correction, μ is the reduced mass: $\mu = m/2$ for the adsorbate–adsorbate interactions, whereas $\mu = m$ for the adsorbate–adsorbent interactions, where m is mass of the adsorbate molecule.

Simulation Methods. Grand canonical Monte Carlo (GCMC) simulations were employed to calculate the adsorption of H_2, CO_2, CH_4, and N_2 in PCN-26. Similar to previous works,[59−62] PCN-26 was treated as rigid framework with atoms frozen at their crystallographic positions, since the effects of the dynamics of MOFs become significant only when the guests are large and/or strong guest–host interactions exist in the system. The simulation box contains 3 (3 × 1 × 1) unit cells, and no finite-size effects existed by checking the simulations with larger boxes. The LJ interactions were calculated with a cutoff distance, 1.28 nm, and the long-range electrostatic interactions were handled using the Ewald summation technique with tinfoil boundary condition. For each state point, the number of steps in

GCMC simulation was 2×10^7, where the first 1×10^7 steps were used for equilibration and the subsequent 1×10^7 steps for sampling the desired thermodynamics properties. A detailed description of the simulation methods can be found elsewhere.[63]

■ RESULTS AND DISCUSSION

Synthesis and Structure of PCN-26·*xS*. Under solvothermal conditions, a reaction between $CuBr_2$ and H_8TDM in DMF affords green crystals of PCN-26·*xS*, which has a formula
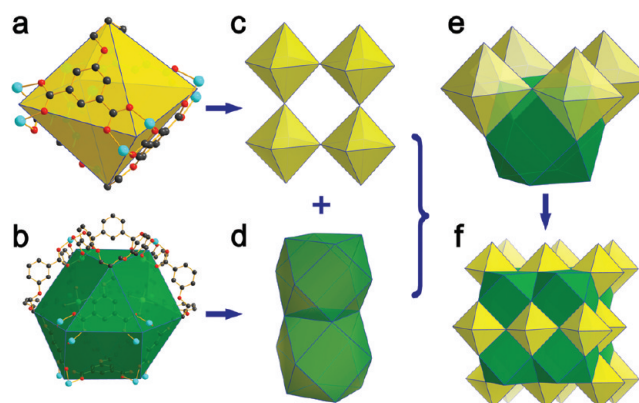
Figure 1. (a) Octahedral cage; (b) cuboctahedral cage; (c) connectivity of octahedrons; (d) connectivity of cuboctahedrons; (e) connectivity of cuboctahedron and neighboring octahedrons; (f) schematic representation of the polyhedron-stacked 3D framework.
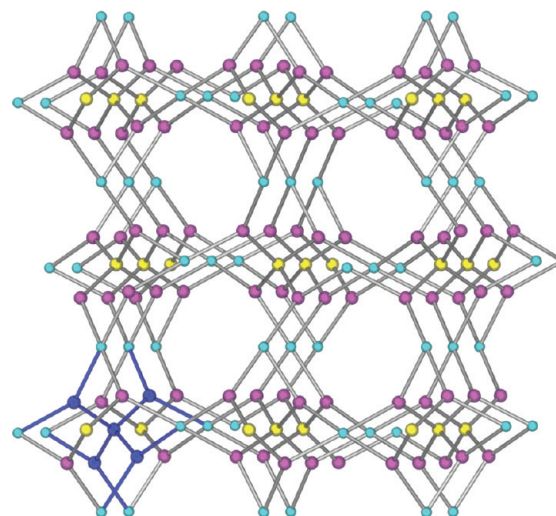
Figure 2. Schematic representation of the topology of PCN-26, in which the $Cu_2(O_2CR)_4$ SBUs (turquoise ball) and quaternary carbon atoms of TDM^{8-} (yellow ball) act as four-connected nodes, whereas the CH_2O-isophthalate groups (purple ball) act as three-connected nodes. The navy blue balls and bonds represent one integrated TDM^{8-}.

of $Cu_4(H_2O)_4(TDM)\cdot xS$. Essentially, the flexibility of free H_8TDM molecule comes from the three single bonds connecting the central carbon and an isophthalate group. Considering the possibility of the flexible configuration of H_8TDM, different synthetic conditions were attempted to explore the possibility of achieving diverse structures. First, $Cu(NO_3)_2$ and $CuCl_2$ were used instead of $CuBr_2$; second, molar ratio of metal salt/ligand (3/1; 2/1; 1/1; 1/2; 1/3) were adjusted; then N,N-diethylformamide (DEF) was introduced to
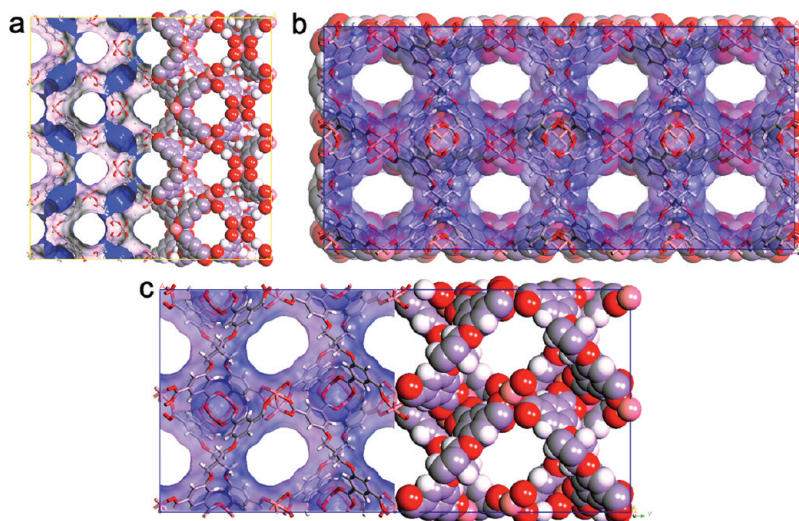
Figure 3. Channels in the framework of PCN-26: (a) along the *a*-axis; (b) along the *b*-axis; and (c) along the *c*-axis.
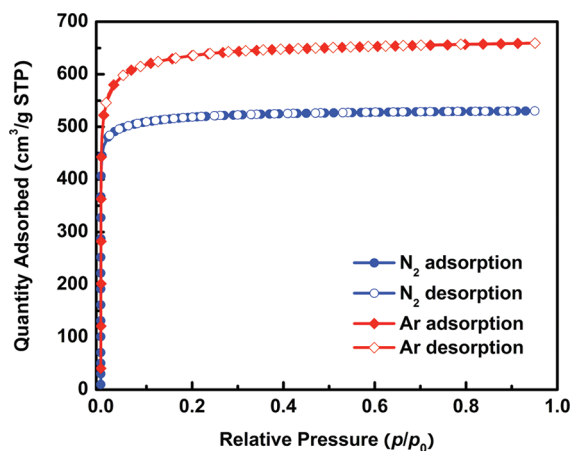

Figure 4. N_2 and Ar isotherms for PCN-26-*ac* at 77 K (filled and open symbols represent adsorption and desorption data, respectively).
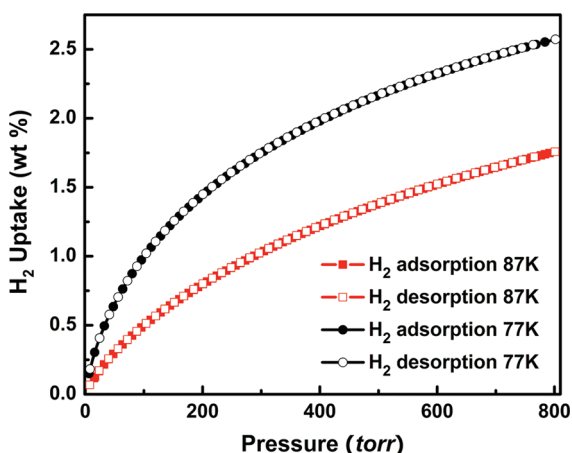

Figure 6. Isosteric heats of adsorption for PCN-26-*ac*.

Figure 5. H_2 isotherms under 77 and 87 K for PCN-26-*ac*.

Figure 7. High-pressure excess H_2 adsorption isotherm at 77 K.

replace DMF. However, PCN-26·*xS* was obtained in all cases, implying a less impact of these changing conditions on the formation of this MOF. Although different solvent molecules involved in the resulting products, the framework structure is identical. In terms of our primary attention on the adsorption-related properties of the MOF, we did not try to identify these
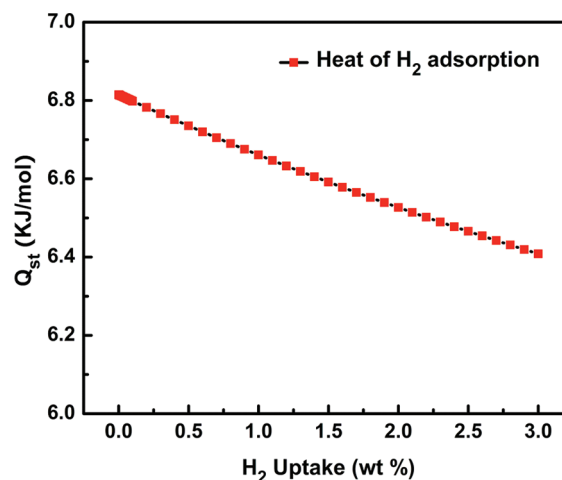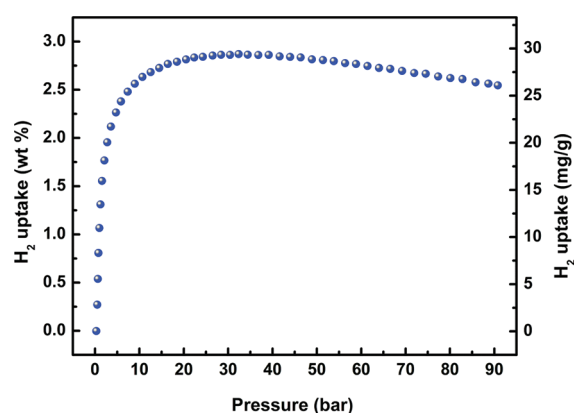
products with different solvent molecules. Herein, the crystal structure of PCN-26 is depicted in detail. Single-crystal X-ray crystallographic analysis[64] revealed that PCN-26 crystallizes in the orthorhombic space group *Pbcm*. In PCN-26, there are two different types of cages. The first type is an octahedral cage, in which four copper paddlewheel SBUs and two quaternary carbon atoms of two TDM[8−] occupy the vertices. The four
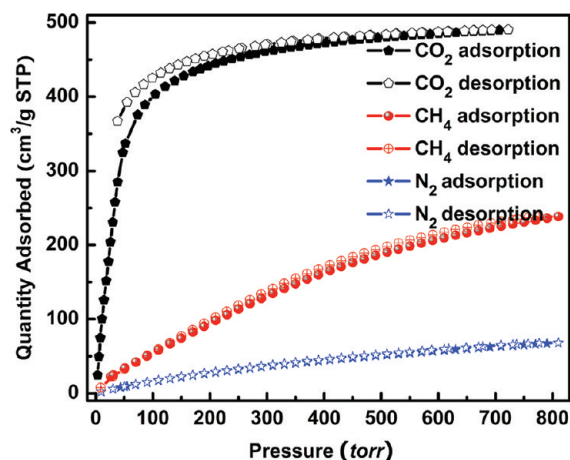
Figure 8. CO_2, CH_4 and N_2 isotherms under 195 K.
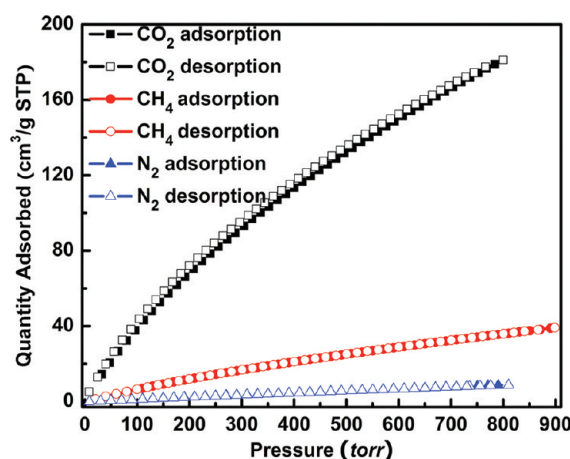
Figure 9. CO_2, CH_4, and N_2 isotherms under 273 K.
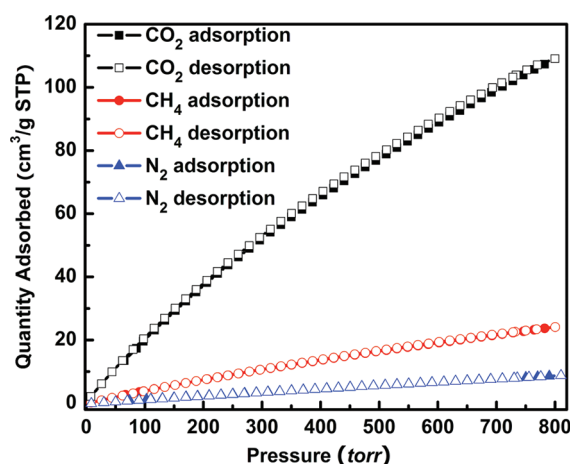
**Figure 10.** CO_2, CH_4, and N_2 isotherms under 298 K.

CH_2O-isophthalate moieties of TDM^{8-} occupied four faces of the octahedral cages, leaving four faces vacant with an isosceles triangle windows of 8.17 Å and 8.82 Å (Cu–Cu and Cu–C distance along the edge; Figure 1a). The second type is a cuboctahedral cage, where eight paddlewheel SBUs and four quaternary carbon atoms occupy the 12 vertices of a cuboctahedron (Figure 1b) and 12 CH_2O-isophthalate parts occupy 12 edges on the outside of the cuboctahedron, whereas

the other 12 edges were occupied by four CH_2O-isophthalate moieties from inside. The square faces are 7.57×7.57 Å^2 and 8.13×8.13 Å^2 in dimension. In three orthogonal directions, each octahedral cage connects six others by sharing the vertices (Figure 1c), whereas every cuboctahedron connects six others by sharing the square faces (Figure 1d). By sharing the corresponding occupied and unoccupied isosceles triangle faces, respectively, each cuboctahedron is surrounded by eight neighboring octahedra (Figure 1e) to form a polyhedron-stacked three-dimensional framework (Figure 1f). It should be pointed out that although the ligand is flexible when stands alone, the resulting MOF is rigid presumably due to the rigidity of the 3D framework structure. Similar situation has been observed in several other MOFs.[65] A change in conformation originating from rotation around a single bond would be energetically unfavorable in the framework because the bonds are all interconnected.

In PCN-26, both $[Cu_2(O_2CR)_4]$ SBUs and quaternary carbon atoms of TDM^{8-} act as four-connected nodes, while the CH_2O-isophthalate moieties act as three-connected nodes, the framework is a trinodal net and adopts a new network topology with the Schläfli symbol of $\{3^{11}.4^{10}.5^7\}_4\{3^2.6^2.7^2\}_2\{3^6\}^{66}$ (Figure 2). Three-dimensional square channels are observed from the a, b and c axis with the sizes of 7.57×7.57 Å^2, 8.13×8.13 Å^2 and 7.93×7.93 Å^2, respectively (Figure 3). After removal of the coordinated solvent molecules, activated PCN-26 was obtained with a solvent accessible volume of 66.2% (calculated using PLATON[45]). PXRD confirmed the phase purity of the bulk samples (PCN-26·xS), as shown in Figure S2 in the Supporting Information. Inside the channels of PCN-26·xS, lie crystallographically disordered solvent molecules. TGA analysis (see Figure S3 in the Supporting Information) showed that as synthesized PCN-26·xS lost 38% weight because of solvent molecules, and the framework decomposed at temperatures above 290 °C.

Gas Sorption. To investigate the permanent porosity of PCN-26, we performed gas sorption experiments for N_2, Ar, H_2, CO_2, and CH_4. The freshly prepared PCN-26·xS crystals were fully activated to obtain PCN-26-ac sample according to the procedure reported in our previous work.[67,68] A careful examination of the PXRD data of the activated samples reveals that PCN-26-ac keeps its crystallinity and framework structure upon activation (see Figure S3 in the Supporting Information). The N_2 sorption isotherms, as shown in Figure 4, reveal that PCN-26-ac exhibits typical type I sorption behavior, a characteristic of microporous materials, which is coincidental with the crystal structure. Derived from the N_2 adsorption data, the Langmuir surface area of PCN-26-ac is 2385 m^2/g, corresponding to a BET surface area of 1733 m^2/g and a total pore volume of 0.84 cm^3/g. The former is smaller than the solvent-accessible surface area estimated based on the crystal structure (2976 m^2/g using a probe of 3.68 Å in diameter) using Materials Studio 5.0.[69] Comparing with N_2 sorption isotherms, the Ar sorption isotherms display a Langmuir surface area of 2545 m^2/g and a BET surface area of 1854 m^2/g (Figure 4). The corresponding total pore volume is 0.84 cm^3/g, which is consistent with that from N_2 adsorption data.

Low-pressure H_2 sorption isotherms at 77 K were collected as well to evaluate its H_2 adsorption performance. PCN-26-ac adsorb 2.57 wt % H_2 gas at 77 K and 760 Torr (Figure 5), comparable to reported results.[67,70−72] To estimate the heats of adsorption (Q_{st}) for H_2 in PCN-26-ac, H_2 adsorption isotherms
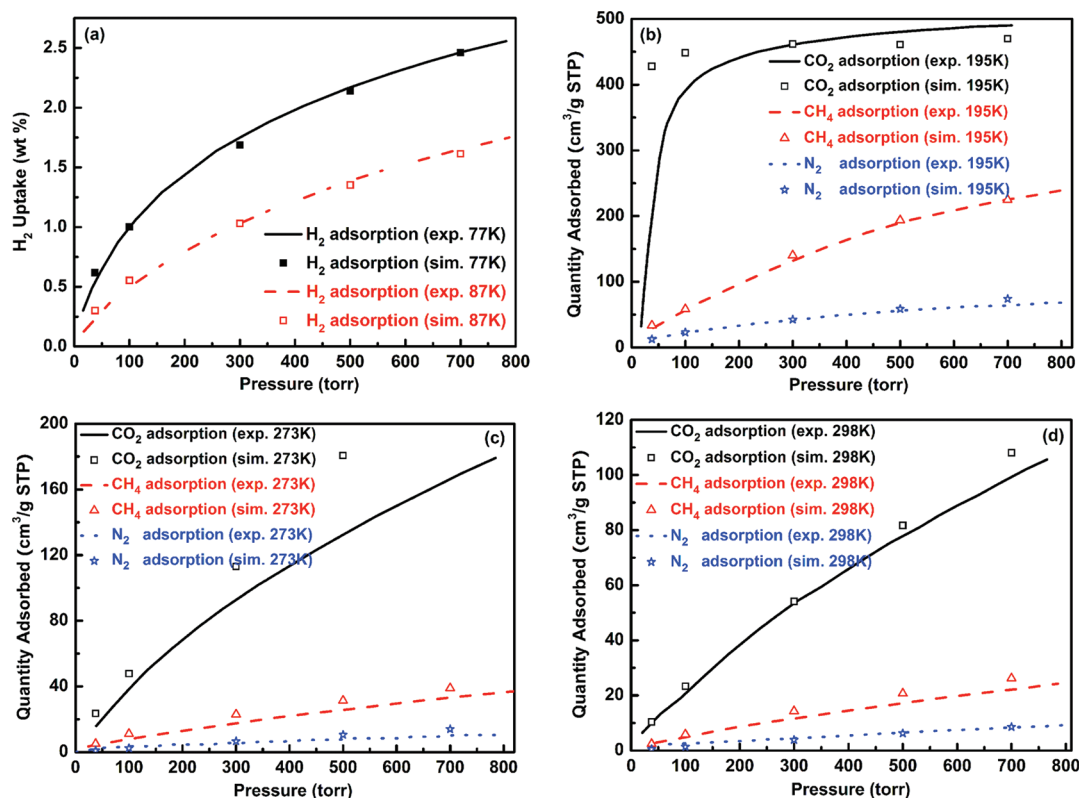
Figure 11. Comparison of experimental and simulated adsorption isotherms of PCN-26-*ac*: (a) H_2 at 77 and 87 K; (b) CO_2, CH_4, and N_2 at 195 K; (c) CO_2, CH_4, and N_2 at 273 K; (d) CO_2, CH_4, and N_2 at 298 K.
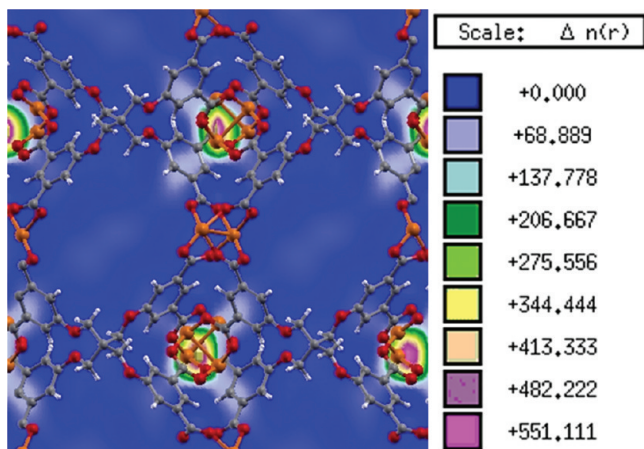
Figure 12. Contour plots of the COM probability densities of CO_2 at 298 K and 37.6 Torr (Cu, orange; O, red; C, gray; H, white).

were measured at 87 K (Figure 5), which adsorb 1.75 wt % H_2 gas. The adsorption data were fitted using the Langmuir–Freundlich equation[73] (utilizing the virial-type expression[7,71] to fit the data could yield similar results), and the heats of adsorption were calculated using the Clausius–Clapeyron equation:[74] $Q_{st} = -Rd(\ln P)/d(1/T)$. As shown in Figure 6, at the low coverage of 0.001 wt %, PCN-26-*ac* has a hydrogen-adsorption enthalpy of 6.81 kJ/mol. These are comparable to the reported Q_{st} of Cu-BTC[71,75] and PCN-6,[76] and can be attributed to the interactions between dihydrogen molecules and open Cu sites as revealed by the recent neutron powder diffraction studies.[77] With the increase in H_2 coverage, Q_{st} of PCN-26-*ac* decreases steadily.

Because the H_2 adsorption isotherm is not saturated at 77 K and 760 Torr, high-pressure H_2 isotherms were collected as well to evaluate its H_2 adsorption performance at elevated pressures. As shown in Figure 7, with the pressure increased to 32.4 bar, the excess gravimetric hydrogen adsorption of PCN-26-*ac* can reach 2.86 wt % at 77 K. The value is relatively lower than those of other reported three-dimensional MOFs[6,70,71,78] under the same conditions, which can be ascribed to the much lower surface area of PCN-26-*ac* compared to those reported MOFs. However, the H_2 uptake capacities of PCN-26-*ac* at 77 K and 1 bar are comparable with those of the MOFs in the literature[67,70–72] and are among the highest for MOFs with flexible ligands at 1 bar.[35,79–83]

Except for the N_2 and H_2 uptakes at low temperatures, CO_2, CH_4, and N_2 adsorption measurements of PCN-26-*ac* have been carried out at 195, 273, and 298 K, respectively (Figures 8–10). At 195 K, PCN-26-*ac* adsorbs CO_2 up to 490.5 cm³/g (753 Torr), CH_4 238.4 cm³/g (809 Torr), and N_2 68.0 cm³/g (810 Torr), respectively. The adsorption capacity for CO_2 can reach 181.3 cm³/g (800 Torr) and for CH_4 39.1 cm³/g (900 Torr), but for N_2 only 8.76 cm³/g (810 Torr) at 273 K. With an increase of temperature to 298 K, the adsorption capacity for CO_2 reaches 109.1 cm³/g (800 Torr) and for CH_4 24.1 cm³/g (800 Torr), but for N_2 only 8.76 cm³/g (810 Torr), as shown in Figure 8. The results demonstrated the guest-evacuated PCN-26-*ac* has the ability to selectively adsorb CO_2 over CH_4 and N_2. To estimate the CO_2/CH_4, CO_2/N_2 adsorption selectivity, the Henry's Law selectivity at 273 and 298 K is calculated.[84] A high CO_2/N_2 selectivity of 49:1 was obtained at 273 K. With an increase in the temperature at 298 K, the CO_2/N_2 selectivity still reaches 21:1. Meanwhile, CO_2/CH_4 selectivity of 8.4:1 and 6.3:1 were obtained at 273 and 298

K, respectively. The gas-adsorption selectivity of PCN-26 is higher than most of the reported values for MOF materials.[85−88]

Comparison of Experimental and Simulated Adsorption Isotherms. The results in Figure 11 show that the simulations give good reproduction of the experimental adsorption isotherms of H_2, CO_2, CH_4, and N_2. Based on these observations, it can be concluded that the set of force fields adopted in this work are reliable and can be used to study the adsorption behaviors of these gases in PCN-26-ac.

Adsorption Sites of CO_2 at 298 K. To investigate the adsorption sites of CO_2 in PCN-26-ac, we calculated the center of mass (COM) probability distribution of the adsorbed CO_2 at low pressure, say 37.6 Torr, on the basis of all of the configurations recorded during the GCMC simulations, as shown in Figure 12. It seems CO_2 molecules are mainly adsorbed in the center of the octahedral cages in the framework. However, it is hard to identify which kind of atoms are the preferential adsorption sites for CO_2. Therefore, the radial distribution functions (RDFs) between each type of atom (shown in Scheme S1 in the Supporting Information) in the framework and the COM of the CO_2 were calculated and the results are reported in Figure S4 in the Supporting Information. This figure shows that the adsorbed CO_2 molecules accumulate mainly in the center of the octahedral cages, and the distances to different atoms are quite close, with the benzene ring and O2 atoms slightly closer.

CONCLUSIONS

The foregoing results have demonstrated that the use of a flexible octatopic ligand as a linker and Cu(II) paddlewheel as a SBU can afford a robust porous 3D MOF with excellent gas-uptake capacity. For instance the MOF can adsorb 2.57 wt % of H_2 (77 K and 760 Torr) and 109.1 cm^3/g of CO_2 (800 Torr and 298 K). Significantly, PCN-26-ac adsorbs CO_2 over CH_4 and N_2 preferably with a CO_2/N_2 selectivity of 49:1 and a CO_2/CH_4 selectivity of 8.4:1 at 273 K. The results of molecular simulation corroborate well with the experimental adsorption isotherms of CO_2, CH_4, and N_2. Additionally, the center of mass (COM) probability distribution of the adsorbed CO_2 at low pressure shows that the adsorbed CO_2 molecules accumulate mainly in the center of the octahedral cages in the framework. Future efforts will be directed toward the study of selective gas uptake of MOFs constructed from other multitopic ligands.

ASSOCIATED CONTENT

Ⓢ Supporting Information

Crystal data in CIF format, thermogravimetry analysis, powder X-ray diffraction patterns, and radial distribution functions of the adsorbed CO_2. These materials are available free of charge via the Internet at http://pubs.acs.org. We acknowledge the Laboratory for Molecular Simulation for providing Materials Studio 5.0 software and Mr. Andrey Yakovenko for powder X-ray studies and analysis.

AUTHOR INFORMATION

Corresponding Author

*E-mail: zhou@mail.chem.tamu.edu. Tel: 1-979-845 4034. Fax:1-979-845 1595.

REFERENCES

(1) Yaghi, O. M.; O'Keeffe, M.; Ockwig, N. W.; Chae, H. K.; Eddaoudi, M.; Kim, J. *Nature* **2003**, *423*, 705−714.
(2) Hong, D. Y.; Hwang, Y. K.; Serre, C.; Ferey, G.; Chang, J. S. *Adv. Funct. Mater.* **2009**, *19*, 1537−1552.
(3) Kitagawa, S.; Kitaura, R.; Noro, S. *Angew. Chem., Int. Ed.* **2004**, *43*, 2334−2375.
(4) Murray, L. J.; Dinca, M.; Long, J. R. *Chem. Soc. Rev.* **2009**, *38*, 1294−1314.
(5) Perry, J. J.; Perman, J. A.; Zaworotko, M. J. *Chem. Soc. Rev.* **2009**, *38*, 1400−1417.
(6) Wong-Foy, A. G.; Matzger, A. J.; Yaghi, O. M. *J. Am. Chem. Soc.* **2006**, *128*, 3494−3495.
(7) Dincă, M.; Dailly, A.; Liu, Y.; Brown, C. M.; Neumann, D. A.; Long, J. R. *J. Am. Chem. Soc.* **2006**, *128*, 16876−16883.
(8) Noro, S.; Kitagawa, S.; Kondo, M.; Seki, K. *Angew. Chem., Int. Ed.* **2000**, *39*, 2082−2084.
(9) Lin, X.; Telepeni, I.; Blake, A. J.; Dailly, A.; Brown, C. M.; Simmons, J. M.; Zoppi, M.; Walker, G. S.; Thomas, K. M.; Mays, T. J.; Hubberstey, P.; Champness, N. R.; Schroder, M. *J. Am. Chem. Soc.* **2009**, *131*, 2159−2171.
(10) Gogotsi, Y.; Dash, R. K.; Yushin, G.; Yildirim, T.; Laudisio, G.; Fischer, J. E. *J. Am. Chem. Soc.* **2005**, *127*, 16006−16007.
(11) Jhung, S. H.; Lee, J. H.; Forster, P. M.; Ferey, G.; Cheetham, A. K.; Chang, J. S. *Chem.—Eur. J.* **2006**, *12*, 7899−7905.
(12) Férey, G.; Mellot-Draznieks, C.; Serre, C.; Millange, F.; Dutour, J.; Surblé, S.; Margiolaki, I. *Science* **2005**, *309*, 2040−2042.
(13) Chae, H. K.; Siberio-Pérez, D. Y.; Kim, J.; Go, Y. B.; Eddaoudi, M.; Matzger, A. J.; O'Keeffe, M.; Yaghi, O. M. *Nature* **2004**, *427*, 523−527.
(14) Nelson, A. P.; Farha, O. K.; Mulfort, K. L.; Hupp, J. T. *J. Am. Chem. Soc.* **2009**, *131*, 458−460.
(15) Furukawa, H.; Ko, N.; Go, Y. B.; Aratani, N.; Choi, S. B.; Choi, E.; Yazaydin, A. O.; Snurr, R. Q.; O'Keeffe, M.; Kim, J.; Yaghi, O. M. *Science* **2010**, *329*, 424−428.
(16) Farha, O. K.; Özgür Yazaydın, A.; Eryazici, I.; Malliakas, C. D.; Hauser, B. G.; Kanatzidis, M. G.; Nguyen, S. T.; Snurr, R. Q.; Hupp, J. T. *Nat Chem* **2010**, *2*, 944−948.
(17) Farha, O. K.; Spokoyny, A. M.; Hauser, B. G.; Bae, Y. S.; Brown, S. E.; Snurr, R. Q.; Mirkin, C. A.; Hupp, J. T. *Chem. Mater.* **2009**, *21*, 3033−3035.
(18) Li, J. R.; Kuppler, R. J.; Zhou, H. C. *Chem. Soc. Rev.* **2009**, *38*, 1477−1504.
(19) Ma, S. Q.; Sun, D. F.; Wang, X. S.; Zhou, H. C. *Angew. Chem., Int. Ed.* **2007**, *46*, 2458−2462.
(20) Bhan, A.; Iglesia, E. *Acc. Chem. Res.* **2008**, *41*, 559−567.
(21) Seo, J. S.; Whang, D.; Lee, H.; Jun, S. I.; Oh, J.; Jeon, Y. J.; Kim, K. *Nature* **2000**, *404*, 982−986.
(22) Hu, A. G.; Ngo, H. L.; Lin, W. B. *J. Am. Chem. Soc.* **2003**, *125*, 11490−11491.
(23) Li, G.; Yu, W. B.; Cui, Y. *J. Am. Chem. Soc.* **2008**, *130*, 4582−4583.
(24) Lee, S. J.; Lin, W. B. *Acc. Chem. Res.* **2008**, *41*, 521−537.
(25) Corma, A.; Diaz-Cabanas, M.; Martinez-Triguero, J.; Rey, F.; Rius, J. *Nature* **2002**, *418*, 514−517.
(26) Lin, Z.-J.; Liu, T.-F.; Xu, B.; Han, L.-W.; Huang, Y.-B.; Cao, R. *CrystEngComm* **2011**, *13*, 3321−3324.
(27) Batten, S. R. *J. Solid State Chem.* **2005**, *178*, 2475−2479.
(28) Cairns, A. J.; Perman, J. A.; Wojtas, L.; Kravtsov, V. C.; Alkordi, M. H.; Eddaoudi, M.; Zaworotko, M. J. *J. Am. Chem. Soc.* **2008**, *130*, 1560−1561.

(29) Bradshaw, D.; Claridge, J. B.; Cussen, E. J.; Prior, T. J.; Rosseinsky, M. J. *Acc. Chem. Res.* **2005**, *38*, 273−282.

(30) Eddaoudi, M.; Moler, D. B.; Li, H. L.; Chen, B. L.; Reineke, T. M.; O'Keeffe, M.; Yaghi, O. M. *Acc. Chem. Res.* **2001**, *34*, 319−330.

(31) Li, H. L.; Davis, C. E.; Groy, T. L.; Kelley, D. G.; Yaghi, O. M. *J. Am. Chem. Soc.* **1998**, *120*, 2186−2187.

(32) Kondo, M.; Okubo, T.; Asami, A.; Noro, S.; Yoshitomi, T.; Kitagawa, S.; Ishii, T.; Matsuzaka, H.; Seki, K. *Angew. Chem., Int. Ed.* **1999**, *38*, 140−143.

(33) Chui, S. S. Y.; Lo, S. M. F.; Charmant, J. P. H.; Orpen, A. G.; Williams, I. D. *Science* **1999**, *283*, 1148−1150.

(34) Wong-Foy, A. G.; Lebel, O.; Matzger, A. J. *J. Am. Chem. Soc.* **2007**, *129*, 15740−15741.

(35) Zhuang, W. J.; Ma, S. Q.; Wang, X. S.; Yuan, D. Q.; Li, J. R.; Zhao, D.; Zhou, H. C. *Chem. Commun.* **2010**, *46*, 5223−5225.

(36) Ma, L.; Lin, W. *J. Am. Chem. Soc.* **2008**, *130*, 13834−13835.

(37) Lin, X.; Blake, A. J.; Wilson, C.; Sun, X. Z.; Champness, N. R.; George, M. W.; Hubberstey, P.; Mokaya, R.; Schröder, M. *J. Am. Chem. Soc.* **2006**, *128*, 10745−10753.

(38) Guillou, N.; Livage, C.; Férey, G. *Eur. J. Inorg. Chem.* **2006**, 4963−4978.

(39) Yuan, D. Q.; Zhao, D.; Sun, D. F.; Zhou, H. C. *Angew. Chem., Int. Ed.* **2010**, *49*, 5357−5361.

(40) Zhao, D.; Yuan, D. Q.; Sun, D. F.; Zhou, H. C. *J. Am. Chem. Soc.* **2009**, *131*, 9186−9188.

(41) Ma, L. Q.; Mihalcik, D. J.; Lin, W. B. *J. Am. Chem. Soc.* **2009**, *131*, 4610−4612.

(42) Tan, C.; Yang, S.; Champness, N. R.; Lin, X.; Blake, A. J.; Lewis, W.; Schroder, M. *Chem. Commun.* **2011**, *47*, 4487−4489.

(43) Rajca, A.; Padmakumar, R.; Smithhisler, D. J.; Desai, S. R.; Ross, C. R.; Stezowski, J. J. *J. Org. Chem.* **1994**, *59*, 7701−7703.

(44) Sheldrick, G. *Acta Crystallogr., Sect. A* **2008**, *64*, 112−122.

(45) Spek, A. L. *J. Appl. Crystallogr.* **2003**, *36*, 7−13.

(46) Marx, D.; Nielaba, P. *Phys. Rev. A* **1992**, *45*, 8968−8971.

(47) Potoff, J. J.; Siepmann, J. I. *AIChE J.* **2001**, *47*, 1676−1682.

(48) Martin, M. G.; Siepmann, J. I. *J. Phys. Chem. B* **1998**, *102*, 2569−2577.

(49) Mayo, S. L.; Olafson, B. D.; Goddard, W. A. *J. Phys. Chem.* **1990**, *94*, 8897−8909.

(50) Frost, H.; Düren, T.; Snurr, R. Q. *J. Phys. Chem. B* **2006**, *110*, 9565−9570.

(51) Frost, H.; Snurr, R. Q. *J. Phys. Chem. C* **2007**, *111*, 18794−18803.

(52) Bae, Y. S.; Mulfort, K. L.; Frost, H.; Ryan, P.; Punnathanam, S.; Broadbelt, L. J.; Hupp, J. T.; Snurr, R. Q. *Langmuir* **2008**, *24*, 8592−8598.

(53) Xu, Q.; Zhong, C. L. *J. Phys. Chem. C* **2010**, *114*, 5035−5042.

(54) Düren, T.; Snurr, R. Q. *J. Phys. Chem. B* **2004**, *108*, 15703−15708.

(55) Karra, J. R.; Walton, K. S. *J. Phys. Chem. C* **2010**, *114*, 15735−15740.

(56) Zheng, C.; Zhong, C. *J. Phys. Chem. C* **2010**, *114*, 9945−9951.

(57) Rappe, A. K.; Casewit, C. J.; Colwell, K. S.; Goddard, W. A.; Skiff, W. M. *J. Am. Chem. Soc.* **1992**, *114*, 10024−10035.

(58) Kumar, A. V. A.; Bhatia, S. K. *Phys. Rev. Lett.* **2005**, *95*, 245901.

(59) Yazaydin, A. O.; Snurr, R. Q.; Park, T. H.; Koh, K.; Liu, J.; LeVan, M. D.; Benin, A. I.; Jakubczak, P.; Lanuza, M.; Galloway, D. B.; Low, J. J.; Willis, R. R. *J. Am. Chem. Soc.* **2009**, *131*, 18198−18199.

(60) Babarao, R.; Jiang, J. W. *J. Am. Chem. Soc.* **2009**, *131*, 11417−11425.

(61) Liu, B.; Smit, B. *J. Phys. Chem. C* **2010**, *114*, 8515−8522.

(62) Xu, Q.; Liu, D. H.; Yang, Q. Y.; Zhong, C. L.; Mi, J. G. *J. Mater. Chem.* **2010**, *20*, 706−714.

(63) Frenkel, D.; Smit, B. *Understanding Molecular Simulation: From Algorithms to Applications*; Academic Press: San Diego, 2002.

(64) PCN-26: C$_{37}$H$_{28}$Cu$_4$O$_{24}$, M = 1110.75, 0.12 × 0.08 × 0.07 mm^3, orthorhombic, space group *Pbcm* (No. 57), a = 12.2473(5), b = 25.914(5), c = 25.9141(9) Å, V = 8224.6(4) Å^3, Z = 4, D_c = 0.897 g/cm^3, F_{000} = 2232, MoKα radiation, λ = 0.71073 Å, T = 173(2)K, $2\theta_{max}$ = 52.8°, 35483 reflections collected, 8349 unique (R_{int} = 0.1352). Final GOF = 0.735, R_1 = 0.0508, wR_2 = 0.0964, R indices based on 3456 reflections with $I > 2\sigma(I)$ (refinement on F^2), 300 parameters, μ = 1.067 mm^{-1}.

(65) Perry, J. J.; Kravtsov, V. C.; McManus, G. J.; Zaworotko, M. J. *J. Am. Chem. Soc.* **2007**, *129*, 10076−10077.

(66) Blatov, V. A. *IUCr CompComm Newslett.* **2006**, *7*, 4−38.

(67) Wang, X. S.; Ma, S. Q.; Rauch, K.; Simmons, J. M.; Yuan, D. Q.; Wang, X. P.; Yildirim, T.; Cole, W. C.; López, J. J.; de Meijere, A.; Zhou, H. C. *Chem. Mater.* **2008**, *20*, 3145−3152.

(68) Ma, S. Q.; Sun, D. F.; Simmons, J. M.; Collier, C. D.; Yuan, D. Q.; Zhou, H. C. *J. Am. Chem. Soc.* **2008**, *130*, 1012−1016.

(69) *Accelrys Materials Studio Release Notes*, version 5.0; Accelrys Software: San Diego, 2008.

(70) Lin, X.; Jia, J. H.; Zhao, X. B.; Thomas, K. M.; Blake, A. J.; Walker, G. S.; Champness, N. R.; Hubberstey, P.; Schröder, M. *Angew. Chem., Int. Ed.* **2006**, *45*, 7358−7364.

(71) Rowsell, J. L. C.; Yaghi, O. M. *J. Am. Chem. Soc.* **2006**, *128*, 1304−1315.

(72) Liu, Y. L.; Eubank, J. F.; Cairns, A. J.; Eckert, J.; Kravtsov, V. C.; Luebke, R.; Eddaoudi, M. *Angew. Chem., Int. Ed.* **2007**, *46*, 3278−3283.

(73) Yang, R. T. *Gas Adsorption by Adsorption Processes*; Butterworth: Boston, 1997.

(74) Roquerol, F.; Rouquerol, J.; Sing, K. *Adsorption by Powders and Solids: Principles, Methodology, and Applications*; Academic Press: London, 1999.

(75) Lee, J. Y.; Li, J.; Jagiello, J. *J. Solid State Chem.* **2005**, *178*, 2527−2532.

(76) Ma, S. Q.; Eckert, J.; Forster, P. M.; Yoon, J. W.; Hwang, Y. K.; Chang, J. S.; Collier, C. D.; Parise, J. B.; Zhou, H. C. *J. Am. Chem. Soc.* **2008**, *130*, 15896−15902.

(77) Peterson, V. K.; Liu, Y.; Brown, C. M.; Kepert, C. J. *J. Am. Chem. Soc.* **2006**, *128*, 15578−15579.

(78) Dincǎ, M.; Han, W. S.; Liu, Y.; Dailly, A.; Brown, C. M.; Long, J. R. *Angew. Chem., Int. Ed.* **2007**, *46*, 1419−1422.

(79) Pachfule, P.; Panda, T.; Dey, C.; Banerjee, R. *Crystengcomm* **2010**, *12*, 2381−2389.

(80) Demessence, A.; Long, J. R. *Chem.—Eur. J.* **2010**, *16*, 5902−5908.

(81) Chun, H.; Seo, J. *Inorg. Chem.* **2009**, *48*, 9980−9982.

(82) Guo, Z. G.; Cao, R.; Wang, X.; Li, H. F.; Yuan, W. B.; Wang, G. J.; Wu, H. H.; Li, J. *J. Am. Chem. Soc.* **2009**, *131*, 6894−6895.

(83) Lee, W. R.; Ryu, D. W.; Lee, J. W.; Yoon, J. H.; Koh, E. K.; Hong, C. S. *Inorg. Chem.* **2010**, *49*, 4723−4725.

(84) Britt, D.; Furukawa, H.; Wang, B.; Glover, T. G.; Yaghi, O. M. *Proc. Natl. Acad. Sci. U.S.A.* **2009**, *106*, 20637−20640.

(85) An, J.; Geib, S. J.; Rosi, N. L. *J. Am. Chem. Soc.* **2010**, *132*, 38−39.

(86) Zhang, Z. J.; Xiang, S. C.; Chen, Y. S.; Ma, S. Q.; Lee, Y.; Phely-Bobin, T.; Chen, B. L. *Inorg. Chem.* **2010**, *49*, 8444−8448.

(87) Zhang, Z.; Xiang, S.; Rao, X.; Zheng, Q.; Fronczek, F. R.; Qian, G.; Chen, B. *Chem. Commun.* **2010**, *46*, 7205−7207.

(88) Park, H. J.; Cheon, Y. E.; Suh, M. P. *Chem.—Eur. J.* **2010**, *16*, 11662−11669.